Journal of Applied Mechanics and Technical Physics, Vol. 41, No. 3, 2000

ANALYSIS OF THE APPLICABILITY OF A MODIFIED KOL'SKII'S METHOD FOR DYNAMIC TESTS OF SOILS IN A DEFORMABLE CASING

V. G. Bazhenov, A. M. Bragov, V. L. Kotov, S. V. Zefirov, A. V. Kochetkov, S. V. Krylov, and A. K. Lomunov

UDC 539.3:624.131

Results of an experimental and theoretical analysis of Kol'skii's method for dynamic tests of soft soils in an elastic casing are presented. The model proposed by S. S. Grigoryan for a plastically compressible medium with parameters determined in shock-wave experiments was used as the model of a soft soil. The high-rate deformation of the soil was simulated using a modified "Dynamics-2" program package. The numerical calculations performed showed that the compliance of the casing and friction practically do not influence the measured characteristics of the soil and the basic premises of Kol'skii's method are adequate for soft soils too.

The behavior of soils under intense dynamic loading is of interest in deriving equations of state, analyzing wave processes in soils, and developing numerical methods for calculating the interaction of land-based and underground structures with soils during strong earthquakes, explosions, and shocks.

The dynamic properties of soils at strain rates of up to 10^2 sec^{-1} have been studied in detail. For higher rates, these properties have been studied inadequately because of the lack of elaborate and well-founded methods for dynamic tests of soils. An effective experimental method for studying the dynamic properties of materials is Kol'skii's method [1]. Bragov et al. [2, 3] proposed a modification of Kol'skii's method that allows one to perform dynamic tests of soils and other loose low-density materials in an elastic casing, to plot strain diagrams, and to determine the lateral-pressure coefficient K_σ. In the papers cited, the feasibility of the basic premises of this method was studied. The present paper is devoted to a numerical analysis of the applicability of this method for testing soils at high strain rates. The dynamic deformation of soils is analyzed using Grigoryan's model of a plastic compressible medium [4]. The validity of the basic premises of Kol'skii's method (uniform stress state in a sample, effects of friction forces and deformability of the casing on wave processes in the system) is assessed from the viewpoint of obtaining reliable characteristics of bulk and shear deformation of soils.

Formulation of the Problem. Mathematical simulation of the high-rate deformation of soft soils in a confining casing is performed in an axisymmetric formulation (Fig. 1), which corresponds to the experimental conditions of [3]. The soil sample 7 is placed in the steel casing 4 between the ends of the loading 8 and reference 6 measurement rods. The steel impactor 1 accelerated in the gas gun barrel impacts the first rod 8 with velocity V_0 and excites in it a plane, one-dimensional, elastic compression wave. Having reached the sample, this wave deforms it. Thus, the wave is partly reflected into the rod 8 as an extension wave and partly propagates in the form of a compression wave through the sample into the reference rod 6. The strain gauge 2 located in the middle of the lateral surface of the loading rod records the longitudinal deformation

Institute of Mechanics, Nizhnii Novgorod State University, Nizhnii Novgorod 603600. Translated from Prikladnaya Mekhanika i Tekhnicheskaya Fizika, Vol. 41, No. 3, pp. 155–162, May–June, 2000. Original article submitted May 18, 1999.

0021-8944/00/4103-0519 $25.00

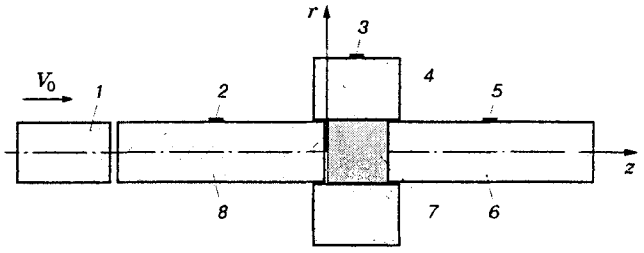

Fig. 1

pulse during passage of the waves transmitted and reflected from the sample, and the strain gauge 5 located in the middle of the reference rod records the deformation pulse transmitted through the sample. The shape of the pulse reflected from the sample characterizes the variation in the strain rate, and integration of the pulse shape yields the development of the deformation of the sample with time. The shape of the pulse transmitted through the sample characterizes the variation in the longitudinal strain component. The strain gauge 3 located on the external surface of the casing records the hoop strain required to determine the lateral pressure of the soil and resistance to shear.

The shock-wave deformation of the system (Fig. 1) is described using a variational-difference procedure [5] based on the dynamic relations for elastoplastic media. The initial system of equations is written in cylindrical coordinates rOz, where the symmetry axis Oz coincides with the rotation axes of the rods and the axis Or ($r \geqslant 0$) is perpendicular to it along the boundary of contact of the first rod with the soil. The variational equation of motion in Lagrangian variables is written in Gurtin's form using the principle of possible motions:

$$\iint_{\Omega} (\sigma_{rr}\delta\dot{e}_{rr} + \sigma_{\theta\theta}\delta\dot{e}_{\theta\theta} + \sigma_{zz}\delta\dot{e}_{zz} + 2\sigma_{rz}\delta\dot{e}_{rz})r\,d\Omega$$
$$- \int_{G} (p_r\delta\dot{u}_r + p_z\delta\dot{u}_z + q_r\delta\dot{u}_r + q_z\delta\dot{u}_z)r\,ds + \iint_{\Omega} \rho(\ddot{u}_r\delta\dot{u}_r + \ddot{u}_z\delta\dot{u}_z)r\,d\Omega = 0.$$

Here σ_{ij} are the stress-tensor components ($i, j = r, z, \theta$), p_α, and q_α are components of the surface load and the contact pressure ($\alpha = r, z$), and ρ is the density; the dots denote differentiation with respect to time. The relationship between the strain-rate tensor and the rate of displacement is derived in the metrics of the current state. Hence, changing the geometry (r and z coordinates) step by step, it is possible to describe large displacements:

$$\dot{e}_{rr} = \dot{u}_{r,r}, \quad \dot{e}_{zz} = \dot{u}_{z,z}, \quad \dot{e}_{\theta\theta} = \dot{u}_r/r, \quad \dot{e}_{rz} = 0.5(\dot{u}_{z,r} + \dot{u}_{r,z}), \tag{1}$$

where the subscript after the comma denotes differentiation with respect to the corresponding variable. Values of the strain-tensor components are determined by integrating the corresponding components of the strain-rate tensor in (1) with respect to time. The relationship between the stress- and strain-tensor components in the elastic rods and the casing is given by Hooke's law.

In the description of the dynamic deformation of the plastically compressible soil, the strain tensor is represented as a superposition of the spherical tensor and the deviator. The spherical stress tensor (pressure) is related to the volumetric strain (density) by the nonlinear law

$$p = \begin{cases} f_1(\rho), & dp/dt > 0, \\ f_2(\rho, \rho^*), & dp/dt \leqslant 0. \end{cases} \tag{2}$$

The first equation in (2) describes the compression curve (shock adiabat) on the active loading segment, and the second equation defines the rarefaction curves from the maximum density attained ρ^*. The corresponding maximum pressure that is reached in the process of shock-compression loading of the particle considered is determined from the shock-adiabatic equation $p^* = f_1(\rho^*)$. If after loading to p^*, the pressure in the particle

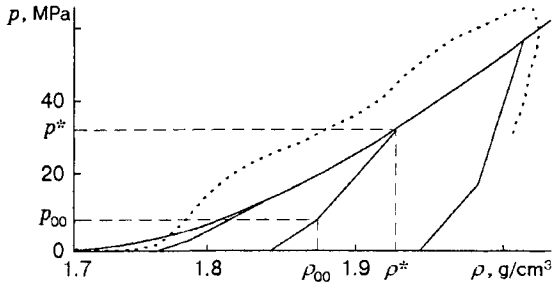

Fig. 2

decreases (rarefaction process), the relation between the pressure and the density is described by the second equation in (2). If the pressure increases again (additional loading), not exceeding p^*, the relation between the pressure and the density is also described by the second equation of (2). Thus, for the particle considered, the parameters p^* and ρ^* can only increase and only under irreversible volumetric strain; they do not vary with elastic changes in the volume.

The shear strains in the soil are described by the plastic flow equations [6]. The components of the strain-rate deviator tensor are defined by $\dot{\varepsilon}_{ij} = \dot{\varepsilon}^e_{ij} + \dot{\varepsilon}^p_{ij}$, where $\dot{\varepsilon}^e_{ij}$ and $\dot{\varepsilon}^p_{ij}$ are the elastic and plastic strains, respectively. The deviator components of the elastic-strain tensor are related to the stress-deviator components by Hooke's law $s_{ij} = 2G\varepsilon^e_{ij}$, where G is the shear modulus. The plastic strains are determined by the associated law of plastic flow $\dot{\varepsilon}^p_{ij} = \lambda s_{ij}$ and the Mises flow condition

$$J_2 = s_{ij}s^{ij}/2 = \sigma_y^2(p)/3, \tag{3}$$

where σ_y is the yield strength, which generally depends on the pressure p and λ is a scalar factor that is proportional to the rate of increase in the plastic-strain work or is equal to zero for elastic deformation [6].

On the surfaces of contact of the rods and the casing with the soil, we impose conditions of nonpenetration along the normal and slip with Coulomb friction in the tangential direction. On the free surfaces of the rods and the casings, stresses are absent. At the impacted end of the rod 8 (Fig. 1), the experimental relation $\sigma_{zz}(t)$ is specified. At the initial time ($t = 0$), the system is at rest and the stresses and strains are equal to zero.

Method of Solution and Calculation Results. The nonlinear wave problem formulated above is solved by an explicit, variational-difference, "cross"-type scheme of the second order of accuracy [5] using the application program package "Dynamics-2" [7]. The rates of displacement and the coordinates of the nodes in the discrete model are determined from the recursive relations

$$\dot{u}_\alpha^{k+1/2} = \dot{u}_\alpha^{k-1/2} + (F_\alpha + Q_\alpha)\frac{\Delta t^{k+1/2}}{F_m}, \quad \alpha^{k+1} = \alpha^k + \dot{u}_\alpha^{k+1/2}\Delta t^{k+1} \quad (\alpha = r,\ z),$$

where F_α and F_m are the generalized nodal forces and mass, Q_α are the contact forces, and Δt^{k+1} is a time step that is close to the Courant number equal to unity relative to the minimum cell size [7].

The units of the experimental setup had the following dimensions: the impactor was 150 mm long and 20 mm in diameter, the measurement rods were 1000 mm long and 20 mm in diameter, the casing had an outside diameter of 42 mm, an inside diameter of 20 m, and a length of 15 mm, and the length of the cylindrical soil sample was 9 mm and its diameter was 20 mm. Calculations were performed for the following mechanical parameters of the rod materials: Young's modulus $E = 185$ GPa, Poisson's constant $\nu = 0.3$, and density $\rho = 7.87$ g/cm^3; for the casing, respectively, $E = 200$ GPa, $\nu = 0.3$, and $\rho = 7.8$ g/cm^3. The impact velocity was $V_0 = 25$ m/sec. The initial density of the soil (sand with a moisture content of 11%) was $\rho_0 = 1.71$ g/cm^3. The shock-adiabatic equation in (2) was defined as [8]

$$f_1(\rho) = M\varepsilon^n,$$

where $\varepsilon = 1 - \rho_0/\rho$ is the volumetric strain, ρ is the current density, $M = 2.1$ GPa, and $n = 1.9$. This relation (solid curve in Fig. 2) approximates the experimental relation $p = \sigma_{zz}(\rho)$ (points in Fig. 2). The function $f_2(\rho, \rho^*)$ in (2) is defined as a two-segment broken line [9]:

$$p = \begin{cases} p^* + C_1^2(\rho - \rho^*), & p > p_{00}, \\ p^* + C_2^2(\rho - \rho^*), & p < p_{00}. \end{cases} \tag{4}$$

Here C_1 and C_2 are the speeds of sound, which determine the slopes to the ρ axis for the first and second links of the broken line (4), respectively, $p_{00} = p^*/\gamma_p$ characterizes the ratio of the lengths of the links of the broken line, (ρ_{00}, p_{00}) is the point of inflection on the rarefaction curve in the (ρ, p) coordinates. The speeds of sound C_1 and C_2 as functions of ρ^* are defined by

$$C_1 = C_0 + \frac{\rho^* - \rho_0}{\rho_g - \rho_0}(C_g - C_0), \qquad C_2 = C_1\Big(1 + \frac{1 - \gamma_c}{\gamma_c}\frac{\rho^* - \rho_0}{\rho_g - \rho_0}\Big). \tag{5}$$

The parameter γ_c specifies the ratio of C_1 to C_2 for $\rho^* = \rho_g$, where ρ_g is the density at which the material becomes similar in properties to a liquid. At the point (ρ_g, p_g), the slope of the first link of the broken line (4) coincides with the slope of the tangent to the shock adiabat in (2). Thus, we have specified the linear variation in C_1 from C_0 to C_g and the linear variation in C_2 from C_0 to C_1/γ_c with variation in the density ρ^* from ρ_0 to ρ_g. Here C_0 is the speed of sound in the soil in the absence of disturbances (or at $\rho = \rho_0$). In the calculations, we set $\gamma_p = 3$, $\gamma_c = 3$, $C_0 = 30$ m/sec, and $\rho_g = 2.5$ g/cm^3. The relation $\sigma_y(p)$ in the yield condition (3) is a nondecreasing function of pressure and is determined from experimental data as follows:

$$\sigma_y(p) = Y_0 + \frac{\mu p}{1 + \mu p/(Y_* - Y_0)}. \tag{6}$$

Here Y_0, μ, and Y_* are the cohesion, the internal-friction coefficient, and the maximum plastic limit, which are equal, respectively, to 0.1, 0.8, and 5.0 MPa. The shear modulus is $G = 5$ MPa and the coefficient of friction of the soil against the surface of the casing is equal to 0.3 [10].

For the measurement rods, we use a grid with 5 cells along the radius and 500 cells along the length. The soil sample is divided into 10 cells along the line of contact with the rods and 9 cells along the line of contact with the casing. The grid of the casing consists of 20×15 cells.

Let us describe briefly the wave processes occurring in the system "impactor–rod 8–soil sample–casing–rod 6 (see Fig. 1). At the moment of impact, an almost one-dimensional compression pulse with a duration of about 70 μsec is formed in the measurement rod. Propagating in the loading rod practically without changes up to the line of contact with the soil sample, this pulse passes in part into the soil and is partly reflected, forming a reflected tension pulse, which is recorded by the gauge 2. Because of the small acoustic rigidity of the soil sample, compared to the acoustic rigidity of the measurement rod, the compression pulse is reflected from the soil as from a free surface, i.e., the pulse is inverted. The pulse transmitted into the soil propagates until interaction with the end of the second measurement rod. The pulse is then reflected from the end and its amplitude increases by a factor of not less than two, which is determined by the nonlinearity of the diagram in the present stress range.

The compression pulse propagates into the rod 6 (see Fig. 1), forming a first local maximum, recorded in the experiment by the gauge 5, and then into the soil sample until reflection from the end of the first rod, where the shock-compression pulse continues to act. The pulse reflected for the second time and having an increased amplitude passes through "soil–rod" interface 6, forming a second maximum. The duration of the compression pulse propagating along the first rod is selected so that after the pulse is reflected for the second time from the sample of soil and approaches the end of the second rod, it is caught up by the rarefaction wave, which propagates with higher velocity and reduces in part the maximum stress in the rod 6. Stresses in the casing arise under the action of the σ_{rr} component of the stress tensor in the soil and the shearing stress σ_{rz} and are recorded by the gauge 3.

In the absence of friction, the stress–strain state of the soil sample cross section is rather uniform. Figure 3 gives curves of $\sigma_{zz}(t)$ in the soil sample at the points $z = 0$ (solid curve), $z = 4.5$ mm (dashed

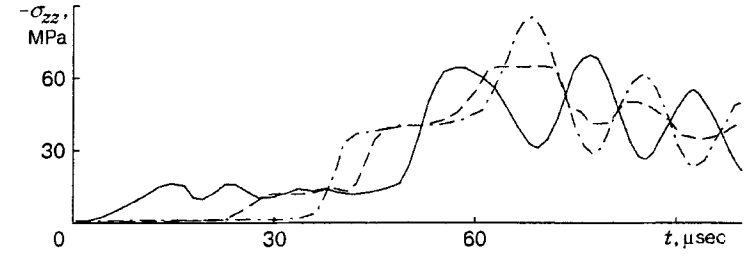

Fig. 3

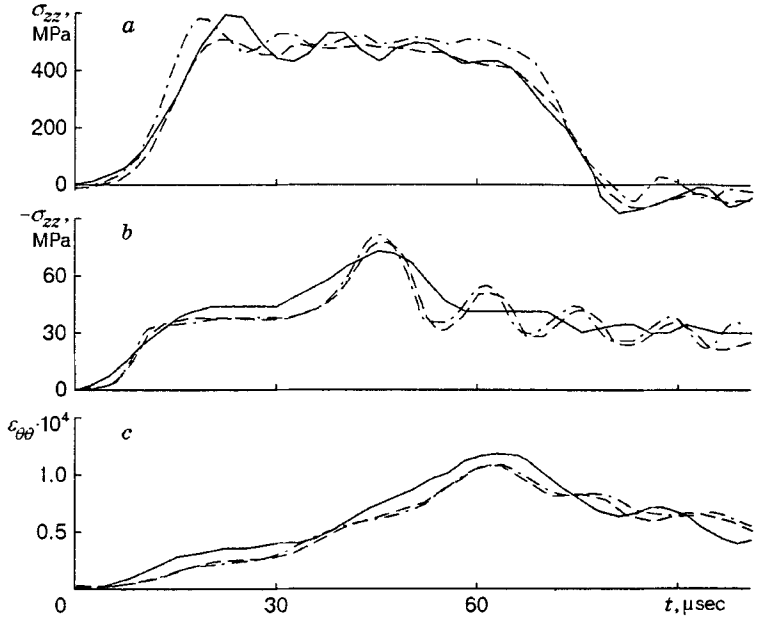

Fig. 4

curve), and $z = 9$ mm (dot-and-dashed curve) at $r = 0$, which practically coincide with the curves at $r = 5$ and 10 mm. Allowance for friction disturbs the uniformity only in a narrow zone adjacent to the boundary of contact of the soil with the casing. Passage of the pulses through the soil layer and repeated reflections from the ends of the rods leads to a nonuniform distribution of the parameters. In this case, it is possible to speak only of the average pressure, which varies with time.

Figure 4 shows experimental (solid) and calculated (dashed) curves of $\sigma_{zz}(t)$ for the reflected pulse recorded by the gauge 2 (Fig. 4a) and the transmitted pulse recorded by the gauge 5 (Fig. 4b) and the hoop strain of the casing $\varepsilon_{\theta\theta}(t)$ recorded by the gauge 3 (Fig. 4c). The time on the curves is measured from the moment the disturbances arrive at the gauges. For comparison with the reflected pulse in Fig. 4a, the dot-and-dashed curve shows the decaying pulse (inverted and displaced in time). Generally, there is satisfactory agreement between the numerical and experimental curves. To estimate the effect of the friction forces, we performed calculations with a friction coefficient equal to zero, which corresponds to ideal slip of the soil relative to the casing and the ends of the rods. The results obtained (dot-and-dashed curves in Fig. 4b and c) indicate that the friction forces have a minor effect on the reflected and transmitted pulses and the hoop strain in the casing, although the hoop-strain gradient along the length of the casing increases. The compliance of the casing also has an insignificant effect on the wave processes in the soil, as follows from a comparison with the solution of the problem for an absolutely rigid casing.

To determine the dynamic strength properties of the soil, it is necessary to determine the lateral load from the side of the soil, which is characterized by the stress component $\varepsilon_{\theta\theta}(t)$, from the hoop strain $\sigma_{rr}(t)$

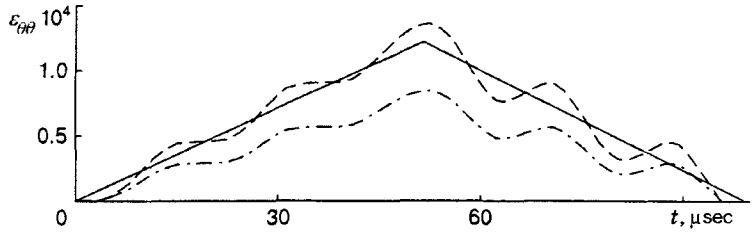

Fig. 5

recorded in the casing. To do this, we use the well-known analytic solution for the stress–strain state of a segment of a thick-walled tube under the action of constant internal pressure. The hoop and radial stresses in a tube with inside diameter a and outside diameter b under the action of internal pressure q are given by the formulas [11]

$$\sigma_{\theta\theta} = A - B/r^2, \qquad \sigma_{rr} = A + B/r^2,$$

where $A = qa^2/(a^2 - b^2)$ and $B = -qa^2b^2/(a^2 - b^2)$. Thus, on the external surface of the segment of the tube, we have

$$\sigma_{rr} = \sigma_{zz} = 0, \qquad \sigma_{\theta\theta} = 2q\,\frac{a^2}{b^2 - a^2}. \tag{7}$$

The hoop strain on the surface of the tube is determined from Hooke's law taking into account (7):

$$\varepsilon_{\theta\theta} = \frac{1}{E}\,\sigma_{\theta\theta} = \frac{2q}{E}\,\frac{a^2}{b^2 - a^2}. \tag{8}$$

Using relation (8) and the hoop strain on the surface of the casing from the experiment of [3], we can calculate the acting internal pressure q:

$$q = \frac{E}{2}\,\frac{b^2 - a^2}{a^2}\,\varepsilon_{\theta\theta}. \tag{9}$$

In the experiment, the role of the internal pressure q is played by the stress σ_{rr} in the soil, and hence, it is possible to obtain the lateral-pressure coefficient $K_\sigma = \sigma_{rr}/\sigma_{zz}$. For stresses between 0 and 50 MPa, the average value of K_σ is 0.5, Poisson's constant is $\nu = K_\sigma/(1 + K_\sigma) = 1/3$, and the average value of the bulk compression modulus is $K = \rho_0 c^2(p) = \rho_0\, df_1(p)/dp = 160$ MPa. The shear modulus G can be determined from the elastic formula $G = 3K(1 - 2\nu)/(2(1 + \nu)) = 3K/8 = 60$ MPa. In the experiment, the load was applied not on the entire surface of the casing since segments 3 mm long on each side were used to align the casing with the measurement rods and they do not contact the soil. To validate formulas (8) and (9), we performed model calculations to determine the stress–strain state of a casing of length $L = 15$ mm with an inside radius of 10 mm and an outside radius of 21 mm under internal load q in the form of a triangular pulse with a length of 100 μsec and a maximum amplitude of 35 MPa, which simulated the real action. In the calculations, we varied the dimension of the region of application of the load l, which coincided with the length of the casing L in the first case and with the length of the sample, equal to 9 mm, in the second case. Results of the test calculation are given in Fig. 5. The solid curve shows the exact solution by formula (7), and the dashed and dot-and-dashed curves show calculations using the program package "Dynamics-2" [7] for $l = 15$ and 9 mm, respectively. It can be seen that the maximum values differ greatly and their difference is proportional to L/l. Thus, to correctly use relations (7) and (9), which define the relation between the hoop strain on the surface of the casing and the soil pressure σ_{rr}, it is necessary to take into account the difference in lengths between the casing and the soil sample.

In addition, we performed a numerical analysis of the propagation of a compression pulse in a system of Hopkinson split rods in the formulation corresponding to the experiment (see Fig. 1), where the length of the casing was 1.7 times greater than the dimension of the soil sample. Ignoring the difference in dimensions

between the casing and the sample soil in determining K_σ, we obtain a value of about 0.5 for the lateral-pressure coefficient in the range of stresses of 0–50 MPa. To satisfy this condition, we use rather larger initial Y_0 and maximum Y_* yield strengths in (6) (40 and 60 MPa, respectively) and $G = 60$ MPa. In the calculations, the coefficient K_σ varied from 0.45 to 0.55, and the hoop strain in the casing was 1.5–2 times smaller than the experimental value. In formula (6), setting $Y_0 = 0.1$ MPa, $Y_* = 5$ MPa, and $G = 5$ MPa, we obtain $K_\sigma \approx 1$. Calculation results for K_σ close to unity are given in Figs. 3 and 4 and agree well with the experimental data.

Thus, to determine the lateral pressure in the soil sample from the hoop strain on the external surface of the casing, it is possible to use formula (9). In this case, the lateral pressure should be calculated taking into account the difference in the dimension of the casing and the sample of soil. To satisfy the condition of a uniform stress–strain state in the soil sample and the casing, it is necessary that the length of the casing be no more than twice the dimension of the cylindrical soil sample ($1 \leqslant L/l \leqslant 2$). If the longitudinal strain in the soil is more than 10%. it is necessary to take into account the change in the loaded part of the casing due to a decrease in the distance between the ends of the measurement rods.

The paper was performed within the framework of the program for supporting the leading scientific schools of Russia (Grant No. 96-15-98156) and the Basic Research Program in the Field of Mining Sciences of the Ministry of Education of the Russian Federation and supported by the Russian Foundation for Fundamental Research (Grant Nos. 97-01-00605 and 99-01-00132).

REFERENCES

1. G. Kol'skii, "Mechanical characteristics of materials at high loading rates," *Mekhanika*, No. 4, 108–119 (1950).
2. A. M. Bragov and G. M. Grushevsky, "Compressibility of soft soils under shock load within the pressure range up to 3 GPa," in: *Wave Processes in Machinery and Structures*: Abstr. of the Europ. Mech. Colloquium Euromech 295 (Nizhnii Novgorod, Russia, Sept. 14–18, 1992), Nizhnii Novgorod (1992), p. 40.
3. A. M. Bragov, V. P. Gandurin, G. M. Grushevskii, and A. K. Lomunov, "New possibilities of Kol'skii's method for studying the dynamic properties of soft soils," *Prikl. Mekh. Tekh. Fiz.*, **36**, No. 3, 179–186 (1995).
4. S. S. Grigoryan, "On the main concepts of the dynamics of soils," *Prikl. Mat. Mekh.*, No. 4, 1057–1072 (1960).
5. V. G. Bazhenov, S. V. Zefirov, and A. I. Kibets, "Numerical realization of the variational-difference moment scheme for solving nonlinear problems of the dynamics of thick shells under pulsed actions," in: *Applied Problems of Strength and Plasticity. Methods of Solution* (collected scientific papers) [in Russian], Izd. Gor'k. Univ., Gor'kii (1988), pp. 66–73.
6. L. M. Kachanov, *Fundamentals of the Theory of Plasticity* [in Russian], Nauka, Moscow (1969), pp. 49–53.
7. V. G. Bazhenov, M. A. Batanin, S. V. Zefirov, et al., "Application program package for solving nonstationary problems of aerohydroelastoplacticity. Complexes of programs for mathematical physics," in: *Proc. VIIth All-Union Seminar on Complexes of Programs of Math. Physics* (Gor'kii, September 8–11, 1981), Inst. of Theor. and Appl. Mech., Sib. Div., Russian Acad. of Sci., Novosibirsk (1982), pp. 216–220.
8. G. V. Rykov, "Experimental study of the stress field in an explosion in sandy soil," *Prikl. Mekh. Tekh. Fiz.*, No. 1, 85–89 (1964).
9. A. A. Vovk, B. V. Zamyshlyaev, L. S. Evterev, et al., *Behavior of Soils under Pulsed Loading* [in Russian], Naukova Dumka, Kiev (1984).
10. N. I. Gerdyukov, A. G. Ioilev, and S. A. Novikov, "Determination of the coefficient of dynamic friction of sandy soil on a rigid wall," *Prikl. Mekh. Tekh. Fiz.*, **36**, No. 4, 185–187 (1995).
11. Yu. N. Rabotnov, *Mechanics of Deformable Solids* [in Russian], Nauka, Moscow (1979), pp. 280–282.